

A Local-Mode Model for Understanding the Dependence of the Extended Amide III Vibrations on Protein Secondary Structure

Thomas Weymuth,[†] Christoph R. Jacob,^{*,†,‡} and Markus Reiher^{*,†}

ETH Zurich, Laboratorium für Physikalische Chemie, Wolfgang-Pauli-Strasse 10, 8093 Zurich, Switzerland, and Karlsruhe Institute of Technology (KIT), Center for Functional Nanostructures, Wolfgang-Gaede-Str. 1a, 76131 Karlsruhe, Germany

Received: May 18, 2010; Revised Manuscript Received: July 6, 2010

The extended amide III region in vibrational spectra of polypeptides and proteins is particularly sensitive to changes in secondary structure. To investigate this structural sensitivity, we have performed density-functional calculations on the small model compound *N*-acetyl-L-alanine-*N*-methylamide, which are analyzed using the recently developed analysis in terms of localized modes [*J. Chem. Phys.* **2009**, *130*, 084106]. We find that the local modes obtained for different backbone conformations are actually rather similar. To probe the secondary structure sensitivity, we investigate the dependence of the local-mode frequencies and coupling constants on the torsional angles ϕ and ψ . This enables us to set up a local-mode model of the extended amide III region for better understanding its structural sensitivity.

1. Introduction

Vibrational spectroscopy is a powerful tool for studying the structure of biomolecules in their natural environment, that is, in aqueous solution. It is applicable in many cases where other techniques, such as nuclear magnetic resonance (NMR) spectroscopy or X-ray crystallography cannot be employed. Infrared (IR) and Raman spectroscopy have in fact extensively been used to gain information about the secondary structure of polypeptides and proteins (for reviews, see, e.g., refs 1–4). However, for large molecules these traditional vibrational spectroscopic techniques often suffer from congested line shapes so that it becomes difficult to extract specific structural information from the spectra. Therefore, specialized vibrational spectroscopic techniques have been developed over the past decades that filter certain information. For instance, ultraviolet (UV) resonance Raman spectroscopy selectively enhances vibrational modes of the peptide backbone,^{5,6} whereas vibrational circular dichroism (VCD)⁷ and Raman optical activity (ROA) spectroscopy⁸ are sensitive to local and global chirality.⁹ In addition, two-dimensional (2D) IR spectroscopy spreads out spectral information over two dimensions and measures anharmonic couplings between vibrations, which also gives access to specific structural information.¹⁰ Since in vibrational spectroscopy the relationship between the observed spectra and the structure is only indirect, quantum chemical calculations are invaluable for interpreting vibrational spectra.¹¹ This is particularly true for the specialized techniques mentioned above, for which reliable rules of thumb are in general lacking (see, e.g., refs 12–14 for recent theoretical studies of ROA spectroscopy of polypeptides and proteins as well as synthetic polymers).

Because of its large sensitivity to changes in secondary structure the extended amide III region, which comprises the spectral range between about 1200 and 1400 cm^{-1} , is of particular interest. In this region one finds the so-called

“classical” amide III vibration (mainly an in-phase combination of the N–H in-plane bending and the C–N stretching vibration, where the ratio between these two could vary) as well as two C α –H bending vibrations (one of which is approximately along the direction of the NC α bond whereas the other one is perpendicular to it). As was first shown by Diem and co-workers by means of isotopic substitution,^{15,16} these modes couple strongly with each other, leading to normal modes which are combinations of the classical amide III vibration and the C α –H bending vibrations. It is generally believed that the pronounced structural sensitivity of the extended amide III region originates from this coupling. Furthermore, in larger polypeptides the modes on different amino acid residues are coupled and the resulting delocalized normal modes further enhance the structural sensitivity of the extended amide III region.

Because of this complexity of the underlying vibrational modes, unraveling the relationship between secondary structure and the extended amide III region of vibrational spectra is significantly more challenging than, for instance, for the rather well-understood amide I band.⁴ Over the past decades, both experimental and quantum chemical studies have tried to address this issue. In a classic paper,¹⁷ Lord proposed that the frequency of the classical amide III vibration depends mainly on the backbone dihedral angle ψ . On the basis of experimental UV resonance Raman data for small model compounds such as *N*-methyl acetamide (NMA), *N*-acetyl-L-alanine-*N*-methylamide, or also a 21 residue polyalanine as well as density-functional theory (DFT) calculations, Asher and co-workers proposed a sinusoidal dependence of the amide III frequency on ψ over the full range of possible angles and an almost negligible linear dependence on ϕ in the range between -95° and -75° .^{18,19} A similar dependence was found by Schweitzer-Stenner et al. in an experimental study on a series of dipeptides.²⁰ Asher and co-workers subsequently refined their model to include effects due to hydrogen bonding and temperature and eventually came up with a semiempirical model relating the frequency of the classical amide III band to the torsional angle ψ .²¹

Such models are, however, to a great extent based on the assumption that the dependence on ϕ is negligible, which is

* To whom correspondence should be addressed. E-mail: christoph.jacob@kit.edu; markus.reiher@phys.chem.ethz.ch.

[†] ETH Zurich, Laboratorium für Physikalische Chemie.

[‡] Karlsruhe Institute of Technology.

only true over the rather small range between -95° and -75° ,^{18,19} whereas values of ϕ outside of this range also occur in the allowed regions of the Ramachandran plot, which mainly cover all negative values of ϕ for α -helices and β -sheets and also include positive values of ϕ if turns or disordered structures are considered. Therefore, for a complete understanding of the extended amide III region, a model based on data obtained for the whole range of both backbone dihedral angles ϕ and ψ is required. However, a DFT study²² trying to relate the frequencies of the classical amide III normal mode of *N*-acetyl-L-alanine-*N*-methylamide to the corresponding values of the backbone dihedral angles based on data gained over their whole range provided not much insight into the structural dependence of the amide III frequencies and only confirmed that the relation between secondary structure and amide III frequencies is difficult to describe. Thus, the current understanding of the structural sensitivity of the extended amide III region remains unsatisfactory.

This is undoubtedly due to the fact that a number of different effects contribute to the structural sensitivity, such as the dependence of the bond strengths on the backbone dihedral angles, the role of the coupling between the classical amide III and C^α -H bending vibrations, and the effect of intra- and intermolecular hydrogen bonding. These are difficult to separate when considering only the frequencies of selected normal modes. Even though it is well-known^{15,16,23} that the coupling of the C^α -H bending vibrations with the classical amide III vibration is of crucial importance for understanding the structural sensitivity of the extended amide III region, most previous studies^{17-20,22} have focused on the amide III frequencies only and largely ignored the C^α -H bending modes.

Moreover, models which solely predict the frequencies of certain vibrational modes provide no information on the normal modes themselves or on their intensities, even though this information is necessary for a complete theoretical description of vibrational spectra. Such empirical models become even more problematic when considering larger polypeptides, where the bands observed in the experimental spectra are due to a larger number of contributing normal modes. In this case, empirical models based on data obtained for small dipeptides might not allow for a reliable extrapolation to larger systems. Instead, models which are able to predict all of the relevant modes in larger polypeptides are required.

A viable alternative is offered by "local models" (local-mode Hamiltonians or vibrational exciton models),²⁴⁻²⁶ which are based on modeling local vibrational modes as well as the couplings between them. Such models have, for instance, been very successful for explaining the amide I band shape in β -sheets^{24,27} and in polypeptides in general^{28,29} as well as for deducing the size and shape of aerosol particles from their IR spectra,^{30,31} and local models have further been explored for predicting amide I ROA spectra in polypeptides.³² Moreover, by including anharmonicities, local-mode models form the basis of interpreting 2D-IR experiments.³³⁻³⁵ Such local models allow for a separation of different effects. For instance, one can expect that intra- and intermolecular hydrogen bonds affect the local modes but not the couplings between them. For the extended amide III region, the dependence of these coupling constants on the backbone dihedral angles can be expected to be rather simple.³⁶ In particular, the couplings between the classical amide III and the C^α -H modes on the same residue in a polypeptide can be expected to depend mainly on ϕ , while the corresponding coupling for groups on adjacent residues is expected to depend on ψ . In addition, such local models provide access not only to

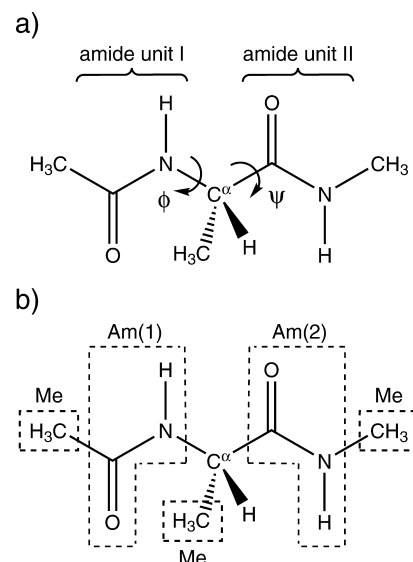


Figure 1. (a) Structure of *N*-acetyl-L-alanine-*N*-methylamide. The two dihedral backbone angles ϕ and ψ are indicated by arrows. (b) Definitions of groups of atoms as used in Table 1.

vibrational frequencies, but also to (models of) the normal modes themselves, and thus allow for a description of intensities. Moreover, local-mode parameters and coupling constants can easily be transferred to larger polypeptides, where they make a full description of all normal modes contributing to the experimentally observed bands possible.

The local-mode parameters and the coupling constants required for such models have so far mainly been obtained from empirical considerations. For the special case of the amide I band, the Hessian matrix reconstruction method by Ham et al. can be employed to extract these parameters from quantum chemical calculations.³⁷ Recently, we developed a methodology for localizing normal modes,³⁸ which determines a unitary transformation that converts a set of normal modes to a set of maximally localized modes. This allows one to extract local-mode parameters and coupling constants from quantum chemical calculations. For the extended amide III region, each resulting localized mode is dominated by the vibration of one single group, and in these localized modes the classical amide III vibration is separated from the C^α -H bending vibrations.³⁶ Thus, the localization of normal modes offers a way to extract a local model of the extended amide III region. In this work, we construct such a model using DFT calculations on *N*-acetyl-L-alanine-*N*-methylamide, shown in Figure 1a. In particular, we investigate how the local mode frequencies and the coupling constants depend on the backbone dihedral angles ϕ and ψ and how hydrogen bonding affects these parameters.

This work is organized as follows. In Section 2 the theoretical methodology is briefly introduced. The vibrational modes in the extended amide III region are discussed in Section 3. The structural dependence of the vibrational frequencies of the local modes and of the coupling constants between them is analyzed in Sections 4 and 5, respectively. These results are then used in Section 6 to construct a local-mode model of the extended amide III region. Finally, conclusions and an outlook are presented in Section 7.

2. Computational Methodology

Within the harmonic approximation, the normal modes and the vibrational frequencies of any molecule can be obtained by diagonalizing the mass-weighted Hessian matrix $H^{(m)}$.^{11,39,40}

TABLE 1: Overview of Mean Values and Standard Deviations of the Contributions of Different Groups of Atoms in *N*-Acetyl-L-alanine-*N*-methylamide to the Extended Amide III Normal Modes and Localized Modes^a

	Me	Am(1)	C ^α -H	Am(2)
mode 1	9.6 ± 3.4	8.7 ± 4.8	77.8 ± 6.4	3.8 ± 4.4
mode 2	11.9 ± 3.5	9.6 ± 7.3	69.6 ± 12.0	8.9 ± 9.6
mode 3	14.3 ± 2.2	48.8 ± 22.4	14.8 ± 9.8	22.1 ± 21.4
mode 4	13.8 ± 2.7	23.6 ± 21.3	11.9 ± 6.2	50.7 ± 21.9
loc. mode C ^α -H(1)	7.2 ± 3.1	7.9 ± 4.7	83.6 ± 4.4	1.4 ± 0.9
loc. mode C ^α -H(2)	14.7 ± 2.4	3.1 ± 2.8	79.5 ± 2.8	2.7 ± 1.1
loc. mode Am III(1)	15.0 ± 1.8	78.9 ± 2.7	5.7 ± 2.8	0.4 ± 0.4
loc. mode Am III(2)	12.7 ± 3.1	0.8 ± 0.6	5.4 ± 3.5	81.0 ± 5.6

^a The individual groups are defined as shown in Figure 1b. For the localized modes, “mode-defining” contributions are set in bold. All values are given in percent.

which contains the second derivatives of the total electronic energy E with respect to the nuclear coordinates,

$$H_{i\alpha,j\beta}^{(m)} = \frac{1}{\sqrt{m_i m_j}} \left(\frac{\partial^2 E}{\partial R_{i\alpha} \partial R_{j\beta}} \right)_0 \quad (1)$$

where m_i is the mass of nucleus i , $R_{i\alpha}$ is the $\alpha = x, y, z$ component of the position vector of nucleus i , and the subscript “0” indicates that the derivatives are evaluated at the equilibrium position. The diagonalization of the Hessian matrix is achieved by the unitary matrix \mathbf{Q} , that is,

$$\mathbf{H}^{(q)} = \mathbf{Q}^T \mathbf{H}^{(m)} \mathbf{Q} \quad (2)$$

where $\mathbf{H}^{(q)}$ is a diagonal matrix of which the diagonal elements are equal to the squares of the normal mode angular frequencies $\omega_p^2 = 4\pi^2 \nu_p^2$, with ν_p being the vibrational frequency of the p -th normal mode. The columns \mathbf{Q}_p of the matrix \mathbf{Q} (i.e., the eigenvectors of the Hessian) are the normal modes in terms of mass-weighted Cartesian coordinates.

For the localization,³⁸ a subset of normal modes is considered, in our case those contributing to the extended amide III region, that is, the four normal modes appearing between 1150 and 1350 cm^{-1} . These are collected in a matrix $\mathbf{Q}^{(\text{sub})}$ and subjected to a unitary transformation \mathbf{U} ,

$$\tilde{\mathbf{Q}}^{(\text{sub})} = \mathbf{Q}^{(\text{sub})} \mathbf{U} \quad (3)$$

to obtain a matrix $\tilde{\mathbf{Q}}^{(\text{sub})}$ which contains the localized modes. The unitary transformation \mathbf{U} is determined such that the resulting modes are maximally localized with respect to a suitably defined localization criterion, for which in this work we employ the atomic-contribution criterion introduced in ref 38. The Hessian matrix given with respect to the localized modes,

$$\tilde{\mathbf{H}}^{(\text{sub})} = \mathbf{U}^T \mathbf{H}^{(q,\text{sub})} \mathbf{U} \quad (4)$$

where the diagonal matrix $\mathbf{H}^{(q,\text{sub})}$ contains the squared angular frequencies of the selected normal modes, is no longer a diagonal matrix. Instead, one can interpret the diagonal elements of $\tilde{\mathbf{H}}^{(\text{sub})}$ as fictitious vibrational frequencies of the localized modes, whereas the off-diagonal elements of $\tilde{\mathbf{H}}^{(\text{sub})}$ represent the couplings between these local modes. It is useful to define the coupling matrix³⁸

$$\tilde{\mathbf{Q}}^{(\text{sub})} = \mathbf{U}^T \mathbf{\Omega}^{(\text{sub})} \mathbf{U} = \frac{1}{2\pi} (\tilde{\mathbf{H}}^{(\text{sub})})^{1/2} \quad (5)$$

where $\mathbf{\Omega}^{(\text{sub})}$ is a diagonal matrix containing the vibrational frequencies of the selected normal modes. The diagonal elements of the coupling matrix $\tilde{\mathbf{Q}}^{(\text{sub})}$ correspond to vibrational frequencies of the localized modes, and the off-diagonal elements correspond to coupling constants given in frequency units.³⁸

All quantum chemical calculations have been performed using DFT with the Turbomole 5.10 program package.⁴¹ The BP86 exchange-correlation functional^{42,43} and Ahlrichs’ valence triple- ζ basis with one set of polarization functions at all atoms (TZVP)⁴⁴ with the corresponding auxiliary basis set^{45,46} were employed. In all calculations, the resolution of the identity (RI) technique^{45,47} was used. The program SNF⁴⁰ was employed for the seminumerical calculation of the molecular Hessian, using Turbomole to calculate the analytic energy gradients. For the vibrational analysis and the localization of normal modes, an add-on package to SNF written in the Python programming language was used.³⁸

Pictures of molecular structures and of normal and localized modes were generated with ChemDraw⁴⁸ and with Jmol,⁴⁹ respectively. The computer algebra system Mathematica 6.0⁵⁰ was employed for the data analysis, least-squares nonlinear regressions, and for plotting wavenumbers and coupling constants.

3. Extended Amide III Vibrational Modes

As the simplest possible model system for studying the extended amide III region, we choose *N*-acetyl-L-alanine-*N*-methylamide (see Figure 1a). It features two amide units, which are connected by the alanine C^α atom. The orientation of the two planar amide units and the C^α-H group with respect to each other is determined by the backbone dihedral angles ϕ (the C-N-C^α-C torsional angle, see Figure 1a) and ψ (the N-C^α-C-N torsional angle, see Figure 1a). To investigate the dependence of the extended amide III vibrations on ϕ and ψ , a grid with a step size of 40° was set up, that is, a total of 81 structures with $\phi, \psi \in \{-160^\circ, -120^\circ, -80^\circ, -40^\circ, 0^\circ, 40^\circ, 80^\circ, 120^\circ, 160^\circ\}$ were considered. For each of these structures, a geometry optimization, in which ϕ and ψ were constrained, has been performed. However, two of these structures, namely, $\phi = 0^\circ, \psi = 0^\circ$ and $\phi = -40^\circ, \psi = 40^\circ$ do not represent sensible conformations due to sterical clashes and were therefore omitted. For each structure, a calculation of the normal modes and their frequencies was performed. Even though the harmonic approximation can in principle only be applied for structures which are stationary points on the potential energy surface, such a procedure is justified if the gradient with respect to the considered normal modes is sufficiently small.⁵¹ For the normal modes considered here, the gradient with respect to the extended amide III normal modes is in all cases smaller than $2.5 \cdot 10^{-3}$ atomic units.

In Figure 2, the calculated IR spectrum of *N*-acetyl-L-alanine-*N*-methylamide is shown for the minimum energy conformation. The extended amide III region, which will be analyzed in the following, is highlighted in this spectrum. Four normal modes are contributing to this region, and we start by studying these extended amide III normal modes. As an example, Figure 3a shows the four relevant normal modes for $\phi = \psi = 160^\circ$ (this geometry has been chosen because for this extended conformation the important atomic displacements are particularly easy to recognize). These modes are ordered according to decreasing wavenumber, starting with the one with the highest wavenumber. The first two normal modes at approximately 1330 and

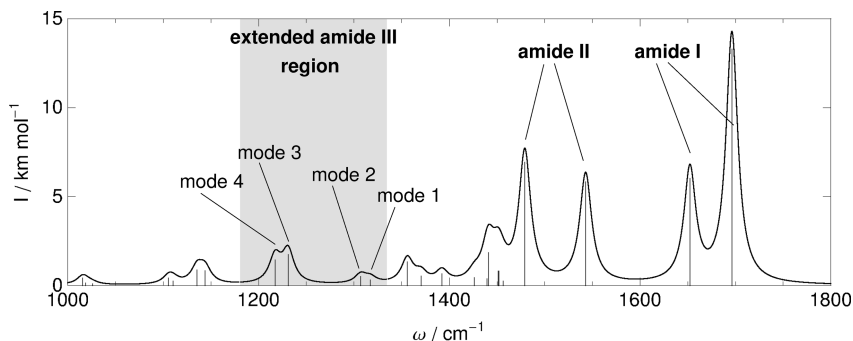


Figure 2. Calculated IR spectrum for the minimum structure ($\phi = -82.6^\circ$ and $\psi = 72.2^\circ$) of *N*-acetyl-L-alanine-*N*-methylamide, with the extended amide III region highlighted in gray. The spectrum has been plotted using a Lorentzian line width of 15 cm^{-1} , and the individual peaks have been included as a line spectrum scaled by 0.04.

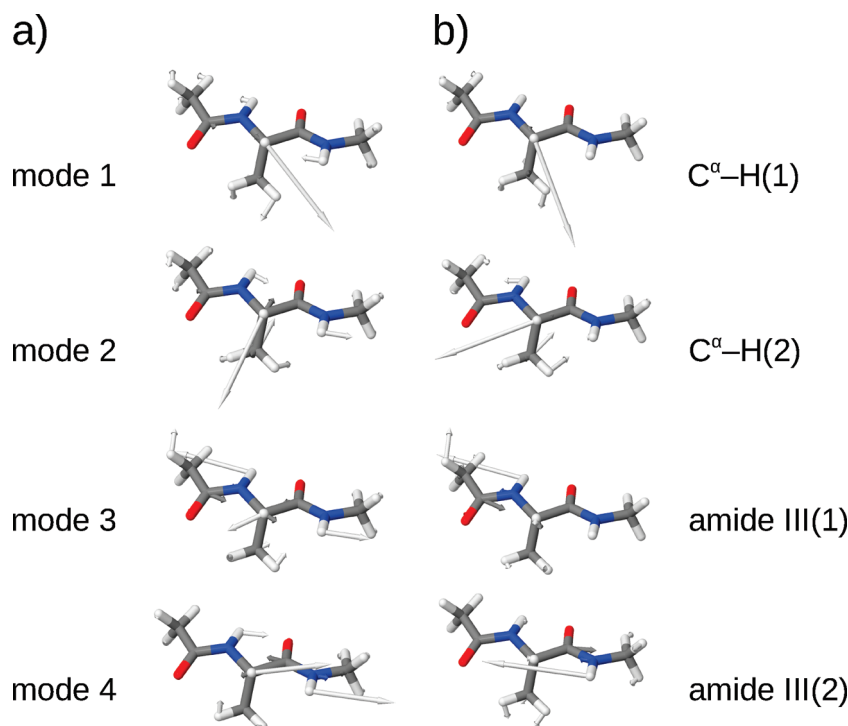


Figure 3. (a) Visualization of the extended amide III normal modes and (b) of the corresponding localized modes for *N*-acetyl-L-alanine-*N*-methylamide in the conformation with $\phi = \psi = 160^\circ$.

1280 cm^{-1} , respectively, are dominated by the two $\text{C}^\alpha\text{-H}$ bending vibrations, with the higher-wavenumber mode being mainly a $\text{C}^\alpha\text{-H}$ bending vibration along the direction of the N-C^α bond, while the lower-wavenumber one features a $\text{C}^\alpha\text{-H}$ bending vibration perpendicular to it. The third and fourth normal modes (appearing at approximately 1220 and 1190 cm^{-1} , respectively) are dominated by the classical amide III vibrations (i.e., an in-phase combination of the N-H bending and C-N stretching vibrations) of the two amide units. Both modes contain contributions from both amide units, and it is further obvious that for both modes there are significant contributions from $\text{C}^\alpha\text{-H}$ bending vibrations. For all normal modes, there are some additional contributions from bending vibrations of the terminal as well as the side-chain methyl groups.

There are quite large differences between the normal modes of different conformations because the degree of mixing between these different vibrations varies. In Table 1 the contributions of groups of atoms (as defined in Figure 1b) to the individual normal modes are reported. The contribution C_{ip} of atom i to normal mode p is calculated as the fraction of the kinetic (or

potential) energy of this atom in the normal mode vibration, which is given by³⁹

$$C_{ip} = \sum_{\alpha=x,y,z} (Q_{i\alpha,p})^2 \quad (6)$$

Note that, because the normal modes are normalized, these atomic contributions will automatically sum to unity. The mean values of the group contributions listed in Table 1 show that in general one vibration dominates the individual normal modes. However, from the rather large standard deviations also included in Table 1, one notices that there are significant differences between normal modes of different conformations. This is particularly obvious for the third and fourth normal modes, for which the contributions of the two amide units vary strongly. In many cases it is not possible to assign the normal modes to a single vibration, and we therefore refrain from classifying the normal modes as amide III(1), amide III(2), $\text{C}^\alpha\text{-H}(1)$, or $\text{C}^\alpha\text{-H}(2)$ vibrations but only label them according to decreasing wavenumbers.

To extract a local-mode model from our calculations, for each structure considered we transformed those four extended amide III normal modes to a set of localized modes (following the terminology introduced in ref 36, these can be referred to as *region-localized modes*). For the example structure considered above, these localized modes are shown in Figure 3b. In contrast to the normal modes, each of these localized modes essentially features one single vibration. There are two localized C $^{\alpha}$ –H bending modes (the first one approximately along the N–C $^{\alpha}$ bond axis, the second one perpendicular to it) as well as two classical amide III vibrations (the first one of the N-terminal amide unit and the second one of the C-terminal amide unit). Except for some admixture of bending vibrations of the methyl groups, these are the only contributions to these localized modes. Nevertheless, it is important to note that the localized modes are not just well-chosen internal coordinates but instead are optimal in the sense that they are as simple as possible and still allow for an exact description of the extended amide III normal modes.

Furthermore, the different local modes are similar for all conformations. This can also be seen when inspecting the group contributions collected in Table 1. For all four localized modes, the contribution of the “mode-defining” vibration is about 80%, and in contrast to the normal modes the standard deviations are relatively small. This is further supported by the overlap between the localized modes obtained for the different conformations (see Supporting Information). For each of the two localized amide III modes, the overlap with the reference mode shown in Figure 3b is in general larger than 0.8, indicating that the amide III localized modes are indeed very similar to each other. For the C $^{\alpha}$ –H bending localized modes, the overlap is rather large (>0.7) in most cases, but there are quite a number of cases where significantly smaller overlaps (sometimes as small as 0.2) are found. This is primarily caused by differences in the direction of the C $^{\alpha}$ –H bending vibration. Since the localization algorithm minimizes the number of atoms contributing to one mode, the direction of the C $^{\alpha}$ –H bending vibration is to some degree arbitrary and can be varied by a rotation among the two localized modes.

4. Structural Dependence of the Mode Frequencies

After having discussed normal modes and localized modes, we now turn to their vibrational frequencies. In Figure 4 the structural dependence of the wavenumbers of each of the four normal modes is shown. For each mode, the plot on the left-hand side shows for fixed values of ϕ the dependence of the wavenumber on ψ , while on the right-hand side the dependence on ϕ is depicted for fixed values of ψ . For the first and second normal mode (both dominated by C $^{\alpha}$ –H bending vibrations), we note a distinct and rather narrow clustering of the wavenumbers around about 1320 and about 1280 cm $^{-1}$, respectively. In the case of the third and fourth mode (dominated by the classical amide III vibrations) the dependence on the torsional angles is stronger, and the wavenumbers span a range of almost 90 cm $^{-1}$. For all modes, one notices that the wavenumbers depend on both dihedral angles and that the form of this dependence is rather difficult. It should be noted that the dependence of wavenumbers of the amide III normal modes on the backbone dihedral angles found in our calculations is qualitatively similar to the one reported in the vibrational frequency map of Mirkin and Krimm,²² even though these earlier calculations used a significantly smaller basis set.

For the structural dependence of the wavenumbers of the localized modes (depicted in Figure 5) one recognizes a similar

situation as in the case of the normal modes. The wavenumbers of the C $^{\alpha}$ –H localized modes span a rather narrow range of about 60 cm $^{-1}$, while the amide III modes span a wider range of approximately 90 cm $^{-1}$. One also notices that the wavenumbers of the two amide III localized modes both mainly cover the same range between approximately 1200 and 1240 cm $^{-1}$.

However, there is a group of 11 structures (marked by black squares in Figure 5) which have considerably higher wavenumbers for the amide III localized modes. One encounters a similar situation in Figure 4 for the third and fourth normal modes. A closer inspection of these 11 structures reveals that they engage in intramolecular hydrogen bonding. Figure 6 plots the wavenumbers of the two amide III localized modes as a function of the distance between the oxygen atom of the first amide unit and the hydrogen atom of the second amide unit. In this figure one can recognize the 11 structures with higher wavenumbers as those for which the O–H distance is smaller than 210 pm. Furthermore, one notices that, for these structures, the wavenumbers of both amide III localized modes are to a good approximation a linear function of this O–H distance. On the other hand, the wavenumbers of the C $^{\alpha}$ –H bending localized modes are not affected by the intramolecular hydrogen bonding. It should be noted that for none of the considered structures the other possible hydrogen bond (i.e., between the hydrogen atom of first amide unit and the oxygen atom of second amide unit) is formed (the corresponding O–H distance being never shorter than 210 pm) and does thus not significantly affect the wavenumbers of the amide III localized modes.

To summarize, we observe that, although the localized modes are much more similar to each other than the normal modes, for their vibrational frequencies this is not the case. For the extended amide III region, similar spreads in wavenumbers are observed for the localized modes and for the corresponding normal modes. For both the normal modes and the localized modes, there appears to be no simple relationship between the backbone angles ϕ and ψ and the vibrational wavenumbers. Nevertheless, we find that, in the cases where intramolecular hydrogen bonds are formed, this leads to an increase of the wavenumber of the amide III localized mode. This increase depends linearly on the O–H distance in this hydrogen bond.

5. Structural Dependence of the Coupling Constants

In a local-mode model, not only the wavenumbers of the local modes enter, but also the couplings between them. The structural dependence of these coupling constants are presented in Figures 7 and 8. For the four local modes considered here, there are six different coupling constants that will be discussed in the following.

We start with the coupling of the classical amide III vibration of the first amide unit (amide III(1) local mode) with the C $^{\alpha}$ –H bending vibrations. The orientation between the first amide and the C $^{\alpha}$ –H units depends only on the torsional angle ϕ (see Figure 1a), so that it can be expected that the corresponding coupling constants are largely independent of ψ .³⁶ This is confirmed for both the amide III(1)/C $^{\alpha}$ –H(1) coupling constant and for the amide III(1)/C $^{\alpha}$ –H(2) coupling constant (see Figure 7). When varying ψ for constant values of ϕ (plots on the left-hand side of Figure 7), the coupling constants turn out to be almost constant, whereas in the plots on the right-hand side of Figure 7 the lines corresponding to constant values of ψ lie very close to each other. For the amide III(1)/C $^{\alpha}$ –H(1) coupling constant, the dependence on ϕ is also not very strong (varying between approximately 0 and 20 cm $^{-1}$), whereas the amide III(1)/C $^{\alpha}$ –H(2) coupling constant varies between –30 and 20

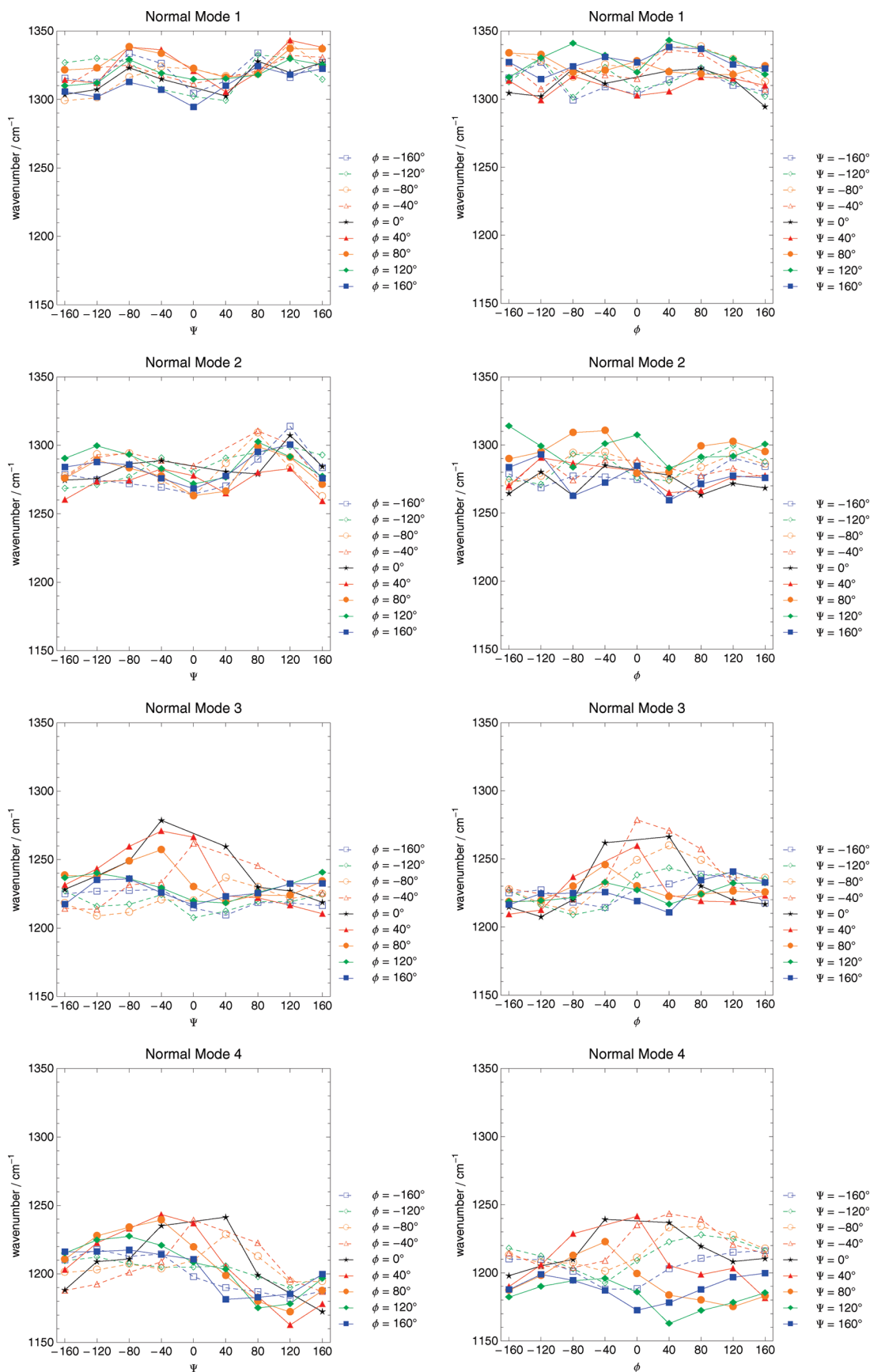


Figure 4. Dependence of the calculated wavenumbers of the normal modes on the dihedral backbone angles ϕ and ψ .

cm^{-1} , with the maximum appearing around $\phi = -40^\circ$ and the minimum at $\phi = \pm 180^\circ$.

For the coupling between the classical amide III vibration of the second amide unit (amide III(2) local mode) with the $\text{C}^\alpha\text{--H}$

bending vibrations, one expects the opposite behavior. Now, the orientation between the groups in question depends solely on ψ , and the corresponding coupling constants should be independent of ϕ . Indeed, for the amide III(2)/ $\text{C}^\alpha\text{--H}$ (1) and

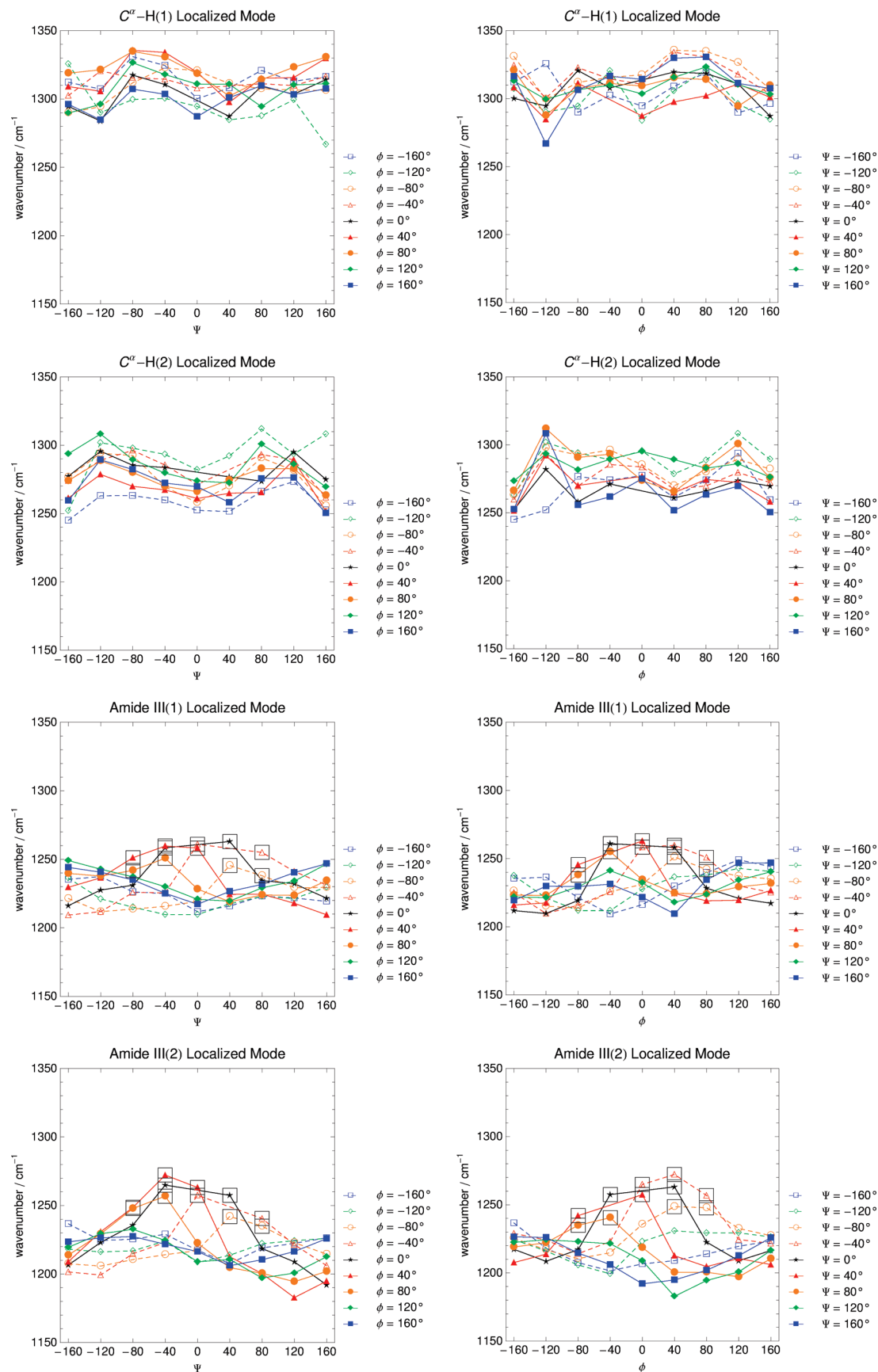


Figure 5. Dependence of the calculated wavenumbers of the localized modes on the dihedral backbone angles ϕ and ψ . For the amide III modes, the black squares mark those structures in which an intramolecular hydrogen bond with an O-H distance smaller than 210 pm is formed.

the amide III(2)/ C^α -H(2) coupling constants, the plots on the left-hand side in Figure 7 show that the lines corresponding to

constant values of ϕ are very close together. For the amide III(2)/ C^α -H(1) coupling constant, which varies between -10 cm⁻¹

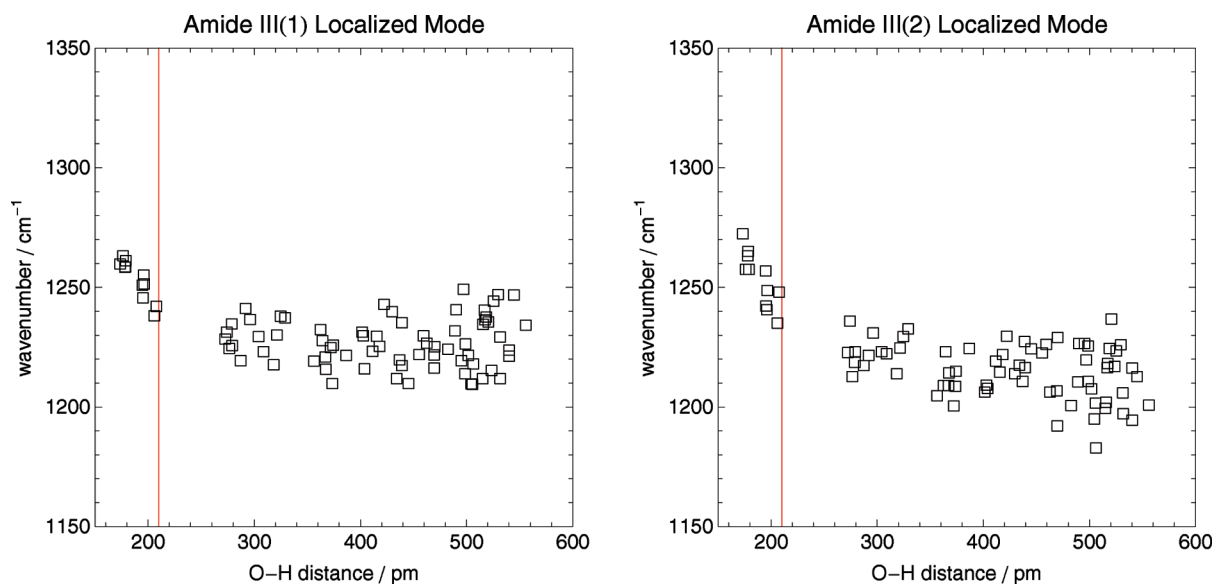


Figure 6. Dependence of the calculated wavenumbers of the amide III localized modes on the distance between the oxygen atom of the first amide group and the hydrogen atom of the second amide group. The vertical red line marks a distance of 210 pm.

and approximately 40 cm^{-1} , one finds a minimum at $\psi \approx -80^\circ$ and a maximum at $\psi \approx \pm 180^\circ$. Similarly, for the amide III(2)/ $\text{C}^\alpha\text{-H}(2)$ coupling constant, varying between -50 cm^{-1} and approximately 10 cm^{-1} , one finds a maximum at $\psi \approx -80^\circ$ and a maximum at $\psi \approx 120^\circ$. However, there are some deviations from an “ideal” behavior, in particular for large values of ψ . Therefore, in the plots on the right-hand side in Figure 7, for a fixed value of ψ the coupling constants as a function of ϕ is not always constant.

The amide III(1)/amide III(2) coupling constant should in principle depend on both dihedral angles, since ϕ as well as ψ changes the relative orientation of the two amide units with respect to each other. However, Figure 8 reveals that this coupling constant seems to depend not so much on ψ , whereas the dependence on ϕ shows a minimum for $\phi = 0^\circ$ and a maximum at $\phi = \pm 180^\circ$. Finally, the $\text{C}^\alpha\text{-H}(1)/\text{C}^\alpha\text{-H}(2)$ coupling constant should depend on neither of the two angles, since in this case both local modes are vibrations of the same set of atoms. While the individual values of this coupling constant mainly cluster around a value of 0 cm^{-1} , one can observe some rather large variations between -30 and 30 cm^{-1} . It should be noted that this coupling constant determines the mixing between the two $\text{C}^\alpha\text{-H}$ bending vibrations, that is, the rotation of the direction of these vibrations, which is not fixed by the localization procedure, and thus is to some degree arbitrary.

In contrast to the localized-mode wavenumbers, we find in most cases for the coupling constants a rather regular dependence on the backbone angles ϕ and ψ . In the cases where the orientation between two coupled local modes depends only on one of these angles, this is reflected in the structural dependence of the corresponding coupling constant, which only depends either on ϕ or ψ . This simple form of the dependence of the coupling constants on ϕ and ψ can easily be parametrized, which will be done in the following section. It should be noted that, in contrast to the wavenumbers of the localized amide III modes, the coupling constants involving these amide III modes are not sensitive to intramolecular hydrogen bonding.

6. Local Mode Model of the Extended Amide III Region

On the basis of the analysis in terms of localized modes and the structural dependence of the local modes and coupling

constants discussed in the previous sections, we now set up a local model of the extended amide III region. For such a model, we aim at simple functions to express both the wavenumbers of the local modes and the coupling constants as functions of ϕ and ψ . Using such a model, it is then possible to set up a coupling matrix $\mathbf{\Omega}$ for any backbone conformation (determined by ϕ and ψ), and the wavenumbers of the normal modes as well as their composition in terms of local modes can be determined by diagonalizing this matrix.

For the wavenumbers of the localized modes we found no simple dependence on the backbone conformation. Therefore, in our model we simply assume local modes that have a constant vibrational frequency. However, for all four localized modes the wavenumbers span quite a broad frequency range. Therefore, treating the wavenumbers as being constant is a rather crude approximation and can be expected to account for quite a large error in the final model. On the basis of a least-squares fit, we use for the local $\text{C}^\alpha\text{-H}(1)$ mode $\tilde{\Omega}_{11} = 1309\text{ cm}^{-1}$, for the local $\text{C}^\alpha\text{-H}(2)$ mode $\tilde{\Omega}_{22} = 1277\text{ cm}^{-1}$, for the local amide III(1) mode $\tilde{\Omega}_{33} = 1227\text{ cm}^{-1}$, and for the local amide III(2) mode $\tilde{\Omega}_{44} = 1215\text{ cm}^{-1}$. For the local amide III modes, we have seen in Section 4 that, when an intramolecular hydrogen bond is formed, the wavenumber linearly depends on the O–H distance of this hydrogen bond. Therefore, if this distance is shorter than 233 or 238 pm, respectively, we apply a correction depending on this O–H distance $d(\text{O-H})$,

$$\tilde{\Omega}_{33} = 1227\text{ cm}^{-1} + 0.61\text{ cm}^{-1} \cdot (233\text{ pm} - d(\text{O-H}))/\text{pm} \quad (7)$$

$$\tilde{\Omega}_{44} = 1215\text{ cm}^{-1} + 0.78\text{ cm}^{-1} \cdot (238\text{ pm} - d(\text{O-H}))/\text{pm} \quad (8)$$

For this linear correction, the slope and the intercept were in both cases determined by a least-squares fit for those structures in which the O–H distance of the intramolecular hydrogen bond is shorter than 210 pm. Note that for the local amide III modes these structures were excluded from the fit determining the average wavenumbers.

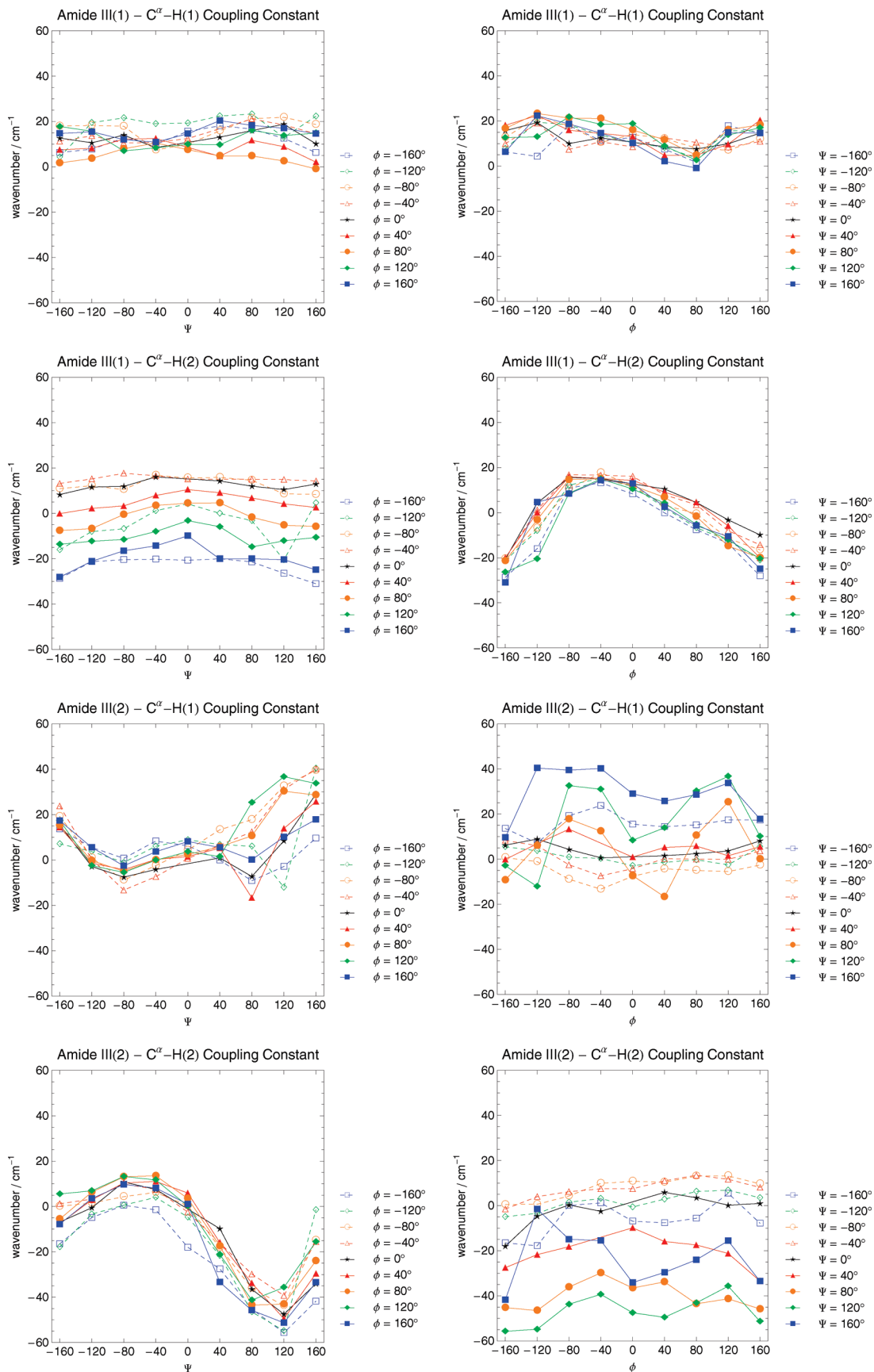


Figure 7. Dependence of the coupling constants of the local modes on the dihedral backbone angles ϕ and ψ .

As discussed in the previous section, the coupling constants in general depend on only one of the backbone angles ϕ and ψ . Therefore, we use a sinusoidal function of the general form $\tilde{\Omega}$

$= a \sin(b + \theta) + c$, where θ is either ϕ or ψ , to describe the dependence of the coupling constants on the backbone conformation. A function of this form is the simplest way to

parametrize the coupling constants such that the correct periodicity with respect to the backbone angles is enforced. The parameters a , b , and c are determined by a nonlinear least-squares fit to the calculated coupling constants. The amide III(1)/C $^{\alpha}$ -H(1) coupling constant $\tilde{\Omega}_{31}$ and the amide III(1)/C $^{\alpha}$ -H(2) coupling constant $\tilde{\Omega}_{32}$ are parametrized to depend only on ϕ as

$$\tilde{\Omega}_{31} = 4.5 \text{ cm}^{-1} \sin(-159^\circ + \phi) + 12.8 \text{ cm}^{-1} \quad (9)$$

$$\tilde{\Omega}_{32} = 18.1 \text{ cm}^{-1} \sin(107^\circ + \phi) - 1.5 \text{ cm}^{-1} \quad (10)$$

whereas the amide III(2)/C $^{\alpha}$ -H(1) coupling constant $\tilde{\Omega}_{41}$ and the amide III(2)/C $^{\alpha}$ -H(2) coupling constant $\tilde{\Omega}_{42}$ are parametrized to depend only on ψ according to

$$\tilde{\Omega}_{41} = 11.8 \text{ cm}^{-1} \sin(-55^\circ + \psi) + 7.9 \text{ cm}^{-1} \quad (11)$$

$$\tilde{\Omega}_{42} = -26.2 \text{ cm}^{-1} \sin(-16^\circ + \psi) - 13.6 \text{ cm}^{-1} \quad (12)$$

The amide III(1)/amide III(2) coupling constant $\tilde{\Omega}_{34}$, for which we found that it mainly depends on ϕ , is parametrized as

$$\tilde{\Omega}_{34} = 9.8 \text{ cm}^{-1} \sin(-87^\circ + \psi) - 4.0 \text{ cm}^{-1} \quad (13)$$

and the C $^{\alpha}$ -H(2)/C $^{\alpha}$ -H(2) coupling constant $\tilde{\Omega}_{12}$, for which no simple structure dependence could be identified, is assumed to be constant with $\tilde{\Omega}_{12} = 5.7 \text{ cm}^{-1}$.

To assess the quality of this model, we calculate the normal mode wavenumbers it predicts for the structures we used for its parametrization and compare them to the calculated ones. We find that the local-mode model reproduces the normal mode wavenumbers with an overall root-mean-square error (RMSE) of 10.9 cm^{-1} . As indicated above, this error mainly originates from the crude approximations made for the local-mode wavenumbers.

One can, of course, ask whether a similar accuracy could have been obtained by fitting the normal mode wavenumbers directly. If we simply fit the normal mode wavenumbers using a constant value for each of them (as we did for the localized modes), this results in an RMSE of 14.6 cm^{-1} , and if we further apply a correction for the formation of intramolecular hydrogen bonds for the third and fourth normal modes, this RMSE is reduced to 11.6 cm^{-1} . Even though these errors are slightly larger than those of our local-mode model, this indicates that for the wavenumbers of the normal modes such a direct fitting leads to similar results. However, our local model offers the advantage to give access to the composition of the normal modes

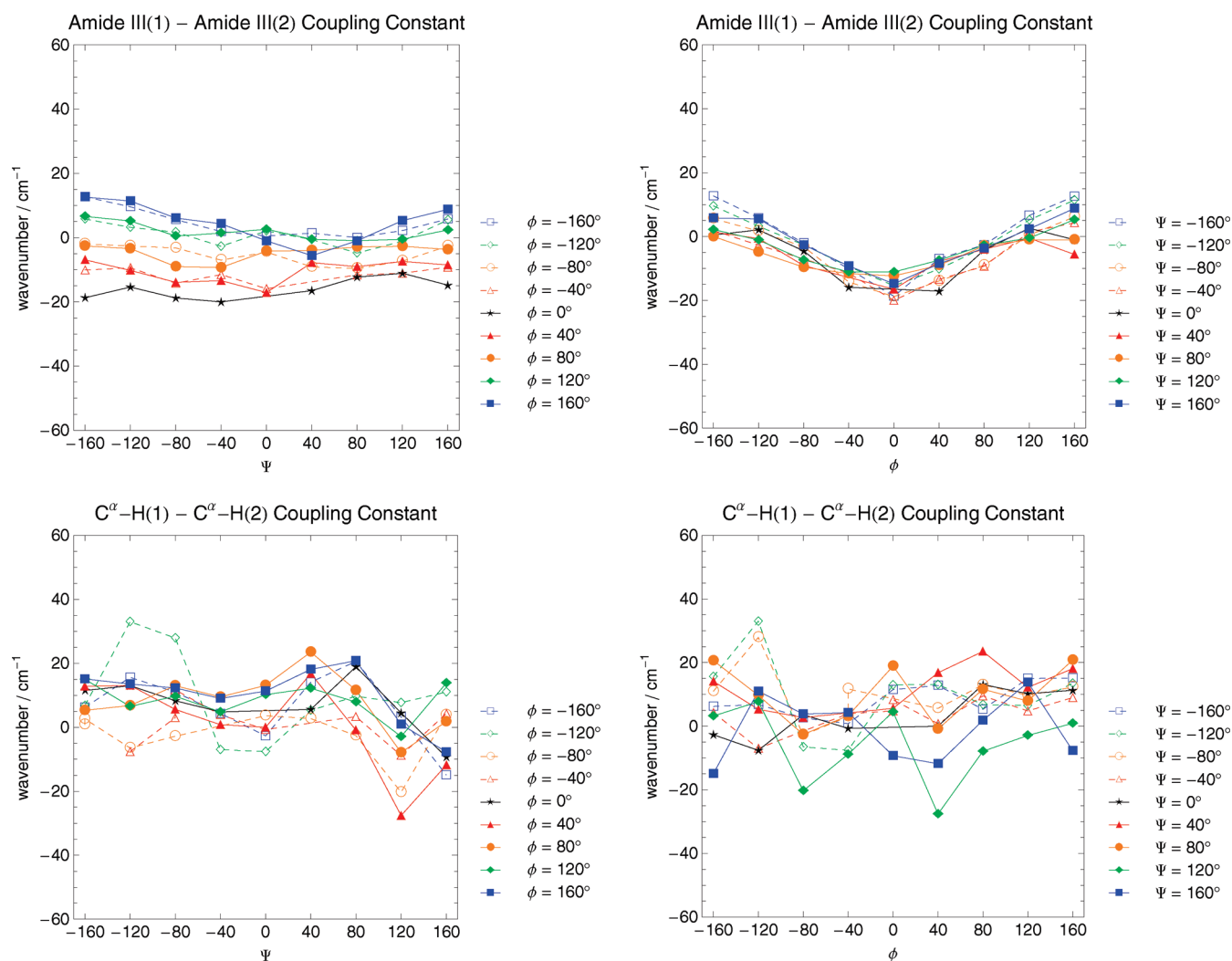


Figure 8. Dependence of the coupling constants of the local modes on the dihedral backbone angles ϕ and ψ .

in terms of local modes and therefore is also suitable for predicting vibrational intensities. Furthermore, it allows for a straightforward extension to larger systems, which is not possible if the normal modes of a model system are fitted directly.

7. Conclusions and Outlook

The extended amide III vibrations in polypeptides and proteins are particularly sensitive to changes in secondary structure. To shed light on this structural dependence, we have performed an analysis of the calculated vibrational spectra of the minimal model system *N*-acetyl-L-alanine-*N*-methylamide in terms of localized modes. On the basis of this analysis, we have parametrized a local-mode model for the extended amide III region. For the considered model system, there are four normal modes in the extended amide III region. These four modes originate both from the “classical” amide III vibrations of the two amide units and from C^α–H bending vibrations. These vibrations mix with each other, leading to rather complex normal modes, which furthermore change significantly when varying the backbone dihedral angles ϕ and ψ . In contrast to this, the localized modes obtained for the extended amide III region are almost pure amide III vibrations of a single amide unit and C^α–H bending vibrations, respectively. Furthermore, the localized modes obtained for different backbone conformations are rather similar to each other. Only for the localized C^α–H bending modes in some cases the direction of the vibration differs because no direction is favored in the localization procedure. Nevertheless, the similarity of the localized modes of different conformations makes it possible to construct a local-mode model in which it is assumed that the local modes are independent of the backbone conformation.

Even though the local modes obtained for different conformations are very similar, this does not hold for their vibrational frequencies. For all four local modes, the wavenumbers vary significantly when the backbone conformation changes. Since this dependence of the local mode wavenumbers on ϕ and ψ does not have a simple form, we simply assume the vibrational frequencies of the localized modes to be constant in our local-mode model and employ an average value for each of them. However, for those structures where intramolecular hydrogen bonds are formed, we find that the wavenumbers of the localized amide III modes are shifted to higher values, with the shift being linearly dependent on the O–H distance of the intramolecular hydrogen bond. A correction term for this shift is included in our local-mode model. It is important to note that the effects of both intra- and intermolecular hydrogen bonds are of utmost importance for modeling the vibrational spectra of polypeptides and proteins, since hydrogen bonds are responsible for stabilizing their secondary structure. From the results obtained here for a model system, it appears that a simple incremental scheme based on hydrogen-bond distances might be sufficient to capture such effects on the localized amide III modes. However, systematic calculations on microsolvated model systems will be necessary to verify this assumption and parametrize such more advanced models.

Besides the local modes and their vibrational frequencies, the couplings between the local modes are an important ingredient of any local-mode model. For these coupling constants we find a much simpler dependence on the backbone conformation. In general, the coupling constants only depend on the dihedral angle that determines the relative orientation of the local modes. In particular, we could confirm that the couplings between the C^α–H and the amide III modes on the same residue in a polypeptide depend only on ϕ , while the corre-

sponding coupling for groups on adjacent residues depends only on ψ . It is further noteworthy that the coupling constants are not sensitive to the formation of hydrogen bonds; that is, for those structures where a significant shift of the wavenumber of the localized amide III mode was found no irregularities are observed for the coupling constants. Only for the coupling between the two localized C^α–H bending vibrations, no simple dependence on the backbone conformation is found. This coupling constant is related to a rotation of the direction of these bending vibrations, and is somehow arbitrary since no preferential direction is enforced in the localization procedure.

By suitably parametrizing the coupling constants, we are able to set up a local-mode model of the extended amide III region. For the model system considered here, this local-mode model is able to reproduce the vibrational frequencies within an RMSE of 10.9 cm⁻¹. This error is similar to what can be achieved by fitting the vibrational frequencies directly. Nevertheless, a local-mode model offers several advantages compared to a direct fit of the normal-mode frequencies of a small model system. First, a local-mode model is not limited to a specific model system, but it can be expected that the local mode parameters and coupling constants are similar also in larger polypeptides and proteins. Therefore, a local-mode model allows for a straightforward extension to larger systems. Second, with a local-mode model it is not only possible to describe the vibrational frequencies, but it also gives access to (models of) the normal modes themselves, which in turn makes it possible to predict vibrational intensities. Particularly for specialized spectroscopic techniques, such as ROA spectroscopy, where reliable rules of thumb are lacking, such simplified models might be of great value for understanding and interpreting experimental spectra.¹² The same applies to 2D-IR experiments, which are commonly interpreted on the basis of local-mode models. However, since such models are usually constructed on the basis of empirical considerations, so far they are restricted to the amide I and amide II bands. The localization procedure applied here makes it possible to construct local-mode models also for more complicated cases, such as for the extended amide III region investigated here, which is a prerequisite for extending 2D-IR spectroscopy to this spectral region.

Of course, the transferability of the model parametrized here to larger polypeptides and proteins has to be investigated in future work. It can be expected that the vibrational frequencies of the local modes will be subject to changes when moving to larger polypeptides, in particular due to the influence of hydrogen bonding. Furthermore, for the central residues in larger polypeptides the local mode frequencies will be very similar, which is in contrast to the small model system considered here where the wavenumbers of the two amide III local modes differ significantly. However, since we found that the coupling between the local modes is not sensitive to changes in the vibrational frequencies, it can be expected that the coupling constants and their parametrization can be applied also to larger polypeptides and proteins. This is what has already been observed for local models of the amide I band.²⁶ Note that, for instance, ROA intensities in the extended amide III region are mainly determined by the coupling between the local modes.¹² Therefore, the coupling constants are much more important than the local mode frequencies. For this reason, it should be possible to develop rules of thumb for the prediction of extended amide III ROA intensities on the basis of the simplified local-mode model developed here. Work in these directions is currently in progress in our group.

Supporting Information Available: Tables of the overlap of normal modes and localized modes calculated for different conformations. This material is available free of charge via the Internet at <http://pubs.acs.org>.

Acknowledgment. C.R.J. acknowledges funding by a Rubicon scholarship of The Netherlands Organization for Scientific Research (NWO) for the time in Zurich as well as from the DFG-Center for Functional Nanostructures in Karlsruhe. This work has been supported by the Swiss National Science Foundation SNF (project 200020-121870).

References and Notes

- Carey, P. R. *J. Biol. Chem.* **1999**, *274*, 26625–26628.
- Thomas, G. J., Jr. *Biopolymers* **2002**, *67*, 214–225.
- Vass, E.; Hollosi, M.; Besson, F.; Buchet, R. *Chem. Rev.* **2003**, *103*, 1917–1954.
- Barth, A. *Biochim. Biophys. Acta* **2007**, *1767*, 1073–1101.
- Schweitzer-Stenner, R. *J. Raman Spectrosc.* **2001**, *32*, 711–732.
- Schweitzer-Stenner, R. *J. Raman Spectrosc.* **2005**, *36*, 276–278.
- Keiderling, T. A. Peptide and Protein Conformational Studies with Vibrational Circular Dichroism and Related Spectroscopies. In *Circular Dichroism: Principles and Applications*, 2nd ed.; Berova, N., Nakanishi, K., Woody, R. W., Eds.; Wiley-VCH: New York, 2000.
- Zhu, F.; Isaacs, N. W.; Hecht, L.; Barron, L. D. *Structure* **2005**, *13*, 1409–1419.
- Herrmann, C.; Ruud, K.; Reiher, M. *ChemPhysChem* **2006**, *7*, 2189–2196.
- Zhuang, W.; Hayashi, T.; Mukamel, S. *Angew. Chem., Int. Ed.* **2009**, *48*, 3750–3781.
- Herrman, C.; Reiher, M. *Top. Curr. Chem.* **2007**, *268*, 85–132.
- Jacob, C. R.; Lubber, S.; Reiher, M. *Chem.—Eur. J.* **2009**, *15*, 13491–13508.
- Luber, S.; Reiher, M. *J. Phys. Chem. B* **2010**, *114*, 1057–1063.
- Liégeois, V.; Jacob, Ch. R.; Champagne, B.; Reiher, M. *J. Phys. Chem. A* **2010**, *114*, 7198–7212.
- Oboodi, M. R.; Alva, C.; Diem, M. *J. Phys. Chem.* **1984**, *88*, 501–505.
- Diem, M.; Lee, O.; Roberts, G. M. *J. Phys. Chem.* **1992**, *96*, 548–554.
- Lord, R. C. *Appl. Spectrosc.* **1977**, *31*, 187–194.
- Asher, S. A.; Ianoul, A.; Mix, G.; Boyden, M. N.; Karnoup, A.; Diem, M.; Schweitzer-Stenner, R. *J. Am. Chem. Soc.* **2001**, *123*, 11775–11781.
- Ianoul, A.; Boyden, M. N.; Asher, S. A. *J. Am. Chem. Soc.* **2001**, *123*, 7433–7434.
- Schweitzer-Stenner, R.; Eker, F.; Huang, Q.; Griebenow, K.; Mroz, P. A.; Kozlowski, P. M. *J. Phys. Chem. B* **2002**, *106*, 4294–4304.
- Mikhonin, A. V.; Bykov, S. V.; Myshakina, N. S.; Asher, S. A. *J. Phys. Chem. B* **2006**, *110*, 1928–1943.
- Mirkin, N. G.; Krimm, S. *J. Phys. Chem. A* **2002**, *106*, 3391–3394.
- Krimm, S.; Bandekar, J. *Adv. Protein Chem.* **1986**, *38*, 181–364.
- Krimm, S.; Abe, Y. *Proc. Natl. Acad. Sci. U.S.A.* **1972**, *69*, 2788–2792.
- Mukamel, S. *Principles of Nonlinear Optical Spectroscopy*; Oxford University Press: New York, 1999.
- Gorbunov, R. D.; Kosov, D. S.; Stock, G. *J. Chem. Phys.* **2005**, *122*, 224904.
- Moore, W. H.; Krimm, S. *Proc. Natl. Acad. Sci. U.S.A.* **1975**, *72*, 4933–4935.
- Torii, H.; Tasumi, M. *J. Chem. Phys.* **1992**, *96*, 3379–3387.
- Brauner, J. W.; Flach, C. R.; Mendelsohn, R. *J. Am. Chem. Soc.* **2005**, *127*, 100–109.
- Firanesco, G.; Signorell, R. *J. Phys. Chem. B* **2009**, *113*, 6366–6377.
- Sigurbjornsson, O. F.; Firanesco, G.; Signorell, R. *Phys. Chem. Chem. Phys.* **2009**, *11*, 187–194.
- Choi, J.-H.; Cho, M. *J. Chem. Phys.* **2009**, *130*, 014503.
- Hamm, P.; Lim, M.; Hochstrasser, R. M. *J. Phys. Chem. B* **1998**, *102*, 6123–6138.
- Ganim, Z.; Chung, H. S.; Smith, A. W.; DeFlores, L. P.; Jones, K. C.; Tokmakoff, A. *Acc. Chem. Res.* **2008**, *41*, 432–441.
- Zhuang, W.; Hayashi, T.; Mukamel, S. *Angew. Chem., Int. Ed.* **2009**, *48*, 3750–3781.
- Jacob, C. R.; Lubber, S.; Reiher, M. *J. Phys. Chem. B* **2009**, *113*, 6558–6573.
- Ham, S.; Cha, S.; Choi, J.-H.; Cho, M. *J. Chem. Phys.* **2003**, *119*, 1451–1461.
- Jacob, C. R.; Reiher, M. *J. Chem. Phys.* **2009**, *130*, 084106.
- Wilson, E. B.; Decius, J. C.; Cross, P. C. *Molecular Vibrations: The Theory of Infrared and Raman Vibrational Spectra*; Dover Publications: New York, 1980.
- Neugebauer, J.; Reiher, M.; Kind, C.; Hess, B. A. *J. Comput. Chem.* **2002**, *23*, 895–910.
- Ahlrichs, R.; Bär, M.; Häser, M.; Horn, H.; Kölmel, C. *Chem. Phys. Lett.* **1989**, *162*, 165–169.
- Becke, A. D. *Phys. Rev. A* **1988**, *38*, 3098–3100.
- Perdew, J. P. *Phys. Rev. B* **1986**, *33*, 8822–8824.
- Schäfer, A.; Huber, C.; Ahlrichs, R. *J. Chem. Phys.* **1994**, *100*, 5829–5835.
- Eichkorn, K.; Treutler, O.; Öhm, H.; Häser, M.; Ahlrichs, R. *Chem. Phys. Lett.* **1995**, *240*, 283–290.
- Eichkorn, K.; Treutler, O.; Öhm, H.; Häser, M.; Ahlrichs, R. *Chem. Phys. Lett.* **1995**, *242*, 652–660.
- Eichkorn, K.; Weigend, F.; Treutler, O.; Ahlrichs, R. *Theor. Chem. Acc.* **1997**, *97*, 119–124.
- ChemDraw Ultra 11.0*; CambridgeSoft: Cambridge, MA, 2008.
- Jmol - An open-source molecule viewer; <http://jmol.sourceforge.net>.
- Mathematica 6.0*; Wolfram Research, Inc.: Champaign, IL, 2007.
- Herrmann, C.; Reiher, M. *Surf. Sci.* **2006**, *600*, 1891–1900.

JP104542W